$$\Delta R = 10\log\left[\frac{1}{\cos^2[\omega t(\rho_i/E_i)^{1/2}]+\frac{1}{4}[(E\rho/E_i\rho_i)^{1/2}+(E_i\rho_i/E\rho)^{1/2}]^2\sin^2[\omega t(\rho_i/E_i)^{1/2}]}\right] \quad (2)$$

Inspection of this equation indicates that the attenuation will be zero decibels whenever the product of the wave number and elastomer thickness is $n\pi$, that is

$$\omega t(\rho_i/E_i)^{1/2} = n\pi \qquad n = 1,2,3,\ldots \quad (3)$$

and that the attenuation will have a maximum value whenever

$$\omega t(\rho_i/E_i)^{1/2} = (2n+1)\pi/2 \qquad n = 1,2,3,\ldots \quad (4)$$

The attenuation for this maximum value may be expressed in decibels as

$$\Delta R_{\max} = 20\log\left|\frac{2(E_i\rho_i E\rho)^{1/2}}{E_i\rho_i+E\rho}\right| \quad (5)$$

The maximum attenuation value is independent of material thickness and frequency for both maximum and minimum values, and the frequency at which it occurs is not dependent on material properties of the base material. Maximum values of attenuation predicted by Eq. (5) for the elastomers in contact with aluminum base material are listed in Table 1. A typical frequency response curve indicates that this resilient layer provides little attenuation for low frequencies and that as the frequency is increased, the maximum and minimum values repeat at integer multiples of the fundamental frequency. This is as expected in accordance with Eqs. (3) and (4).

Since the attenuation curves for the elastomeric materials are periodic between maximum and minimum values, they are not well suited for the attenuation of broad band noise. To overcome this shortcoming, two elastomer discontinuities could be used. These should be designed so that one has its maximum value while the other has its minimum value. In this way, the attenuation would be flat over a rather broad range. These two gaskets should be designed so as to be far enough apart (and separated by sufficient base material) to eliminate any possible dynamic interaction.

In order to select an elastomeric gasket material and thickness which permit maximum heat transfer and minimum vibration transmission, the following procedure would be used. The thermal characteristics are considered first, and the type of material is selected from Fig. 2 for the approximate joint loading. For a compression joint of 200 psi load and a gasket material with a nonmetallic filler, silicone elastomer *C*3 would be selected. The maximum vibration attenuation value ($\Delta R_{\max}$) for elastomer *C*3 is then read from Table 1. Equation (4) may then be used to determine the required thickness of this material for minimum vibration transmission. Once the thickness has been determined, the thermal conductance or effective thermal conductivity of the gasket may then be calculated with Eq. (1) and the bare junction characteristics.‡ The effectiveness of the vibration attenuation in the vicinity of the optimum design may then be determined from Eq. (2). Thus, the heat-transfer requirements give the selection of the material and the vibration requirements determine the thickness.

A technique for the optimum design and selection of elastomeric type gasket materials for combined thermal and vibration performance has been developed. The procedure has been demonstrated for the case of maximum heat transfer and minimum vibration transmission. The technique presented here may also be extended to applications involving the optimum design of gaskets for other materials and conditions.

‡ Effective bare junction thermal conductivity, $h_c\delta_0 = 0.0014P_a + 0.04$.

References

[1] Fletcher, L. S. and Miller, R. G., "Thermal Conductance of Gasket Materials for Spacecraft Joints," *AIAA Progress in Astronautics and Aeronautics: Thermophysics and Spacecraft Thermal Control*, Vol. 35, edited by R. G. Hering, MIT Press, Cambridge, Mass., 1974.

[2] Fletcher, L. S., "A Review of Thermal Control Materials for Metallic Junctions," *Journal of Spacecraft and Rockets*, Vol. 9, No. 12, Dec. 1972, pp. 849–850.

[3] Fletcher, L. S. and Gyorog, D. A., "Prediction of Thermal Contact Conductance Between Similar Metal Surfaces," *AIAA Progress in Astronautics and Aeronautics: Heat Transfer and Spacecraft Thermal Control*, Vol. 24, edited by J. W. Lucas, MIT Press, Cambridge, Mass., 1971, pp. 273–288.

[4] Kenner, V. H. and Goldsmith, W., "One-Dimensional Wave Propagation Through a Short Discontinuity," *Journal of the Acoustical Society of America*, Vol. 45, No. 1, 1969, pp. 115–118.

[5] Beranek, L. L., *Noise and Vibration Control*, McGraw-Hill, New York, 1971, pp. 252–355.

Computer Illustrations of Earth Satellite Orbits

DONALD L. HITZL*

Lockheed Palo Alto Research Laboratory, Palo Alto, Calif.

Introduction

IN most forms of analytical work, there is often a dichotomy between those who rely on clever paper and pencil analysis and those who rely on extensive simulation by computer. However, computer illustrations, which combine rapid visualization with numerical precision, can form a natural bridge between these two viewpoints. Moreover, the importance of visual information in general, and for aerospace applications in particular, should not be underestimated.[1]

As an example of visual results, a set of computer-generated plots are presented which show the orbital motion and ground track for satellites in various Earth orbits. Since most Earth satellite applications involve the orbital motion with respect to some geographical area or location on the Earth's surface, the plots depict satellite motion *relative* to the rotating Earth. The orbits shown are all Keplerian ellipses with prescribed eccentricities and periods. However, as a result of the superimposed rotation of the Earth, the simple two-body motion is distorted in unusual (and sometimes unexpected) ways.

Table 1 Orbit elements

Orbit elements	Orbit period T (hr) 6	8	12	24
semimajor axis a (naut miles)	9046.71	10959.32	14360.79	22796.39
eccentricity[a] e	0.509	0.595	0.5	0.1
inclination i (deg)	63.4	63.4	63.4	63.4
argument of perigee ω (deg)	−90.0	−90.0	−90.0	−90.0
right ascension of ascending node Ω (deg)	−90.0	−90.0	−110.0	90.0
mean anomaly at initial time $M(t_0)$ (deg)	0.0	0.0	35.19	0.0

[a] Note that the eccentricities for the 6- and 8-hr orbits were chosen so perigee altitude would be 1000 naut miles.

Received August 2, 1973; revision received January 15, 1974. Help with the computer program generously given by the late K. Shoop is gratefully acknowledged. This material was developed in the course of satellite systems studies sponsored by the Department of the Air Force.

Index categories: Earth-Orbital Trajectories; Earth Satellite Systems, Unmanned; Computer Technology and Computer Simulation Techniques.

* Research Scientist, Mathematics and Systems Analysis Department. Member AIAA.

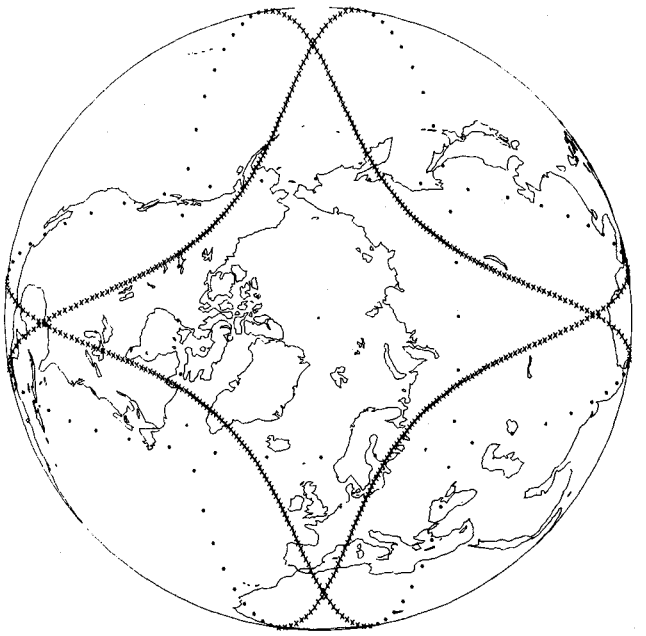

Fig. 1 Ground track for a 6-hr elliptic orbit.

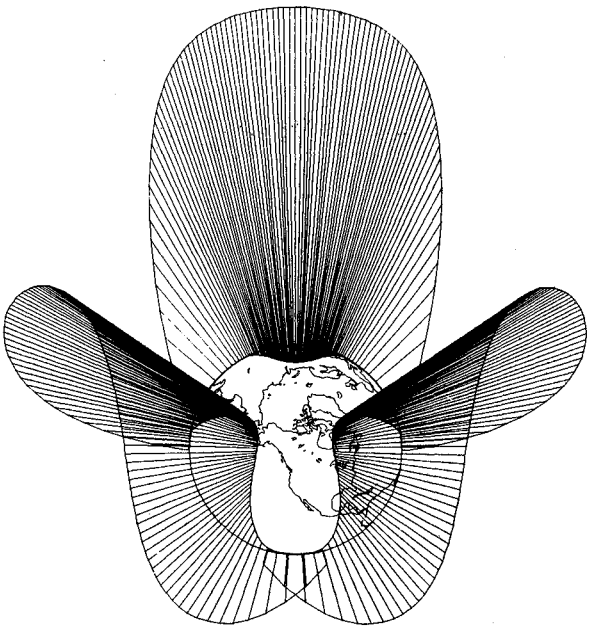

Fig. 3 Northern hemisphere view for an 8-hr elliptic orbit.

The four orbits presented here also have an additional unique characteristic. They were chosen to be subsynchronous—i.e., their periods are commensurate with 24 hr. With this restriction, the orbits generate butterfly-like shapes with a set of symmetric "wings" which close on themselves and repeat after 24 hr have elapsed. These four orbits are defined by their orbital elements given in Table 1.

Illustrations

The illustrations are computed by orthographic projection onto a plane above a given Earth viewpoint. In this way, a degree of three-dimensionality and perspective is achieved in the two-dimensional pictures. Actually, the plots are similar to time lapse photographs of an object in orbit taken by a hypothetical photographer located (permanently!) some distance above a specified Earth location. Figures of this sort can easily provide a wealth of information concerning the somewhat complicated geometry of the relative motion.

Figures 1–5 give representative examples of the types of plots that can be generated. Data describing each plot are given in Table 2. Figure 1 depicts the ground track for four complete orbits of a 6-hr elliptic orbit. Subsatellite points above the equator are marked by x while points below the equator are marked by *. Figure 2 begins the perspective views. Here the four orbital passes of the 6-hr elliptic orbit are shown. Positions in orbit are connected by straight lines with the corresponding subsatellite points. This forms a curtain which gives some perspective to the drawing. Also note that only the visible portions of the orbit and ground track are displayed. Figure 3 shows a similar view for an 8-hr elliptic orbit. Figure 4 gives a view of the relative motion for a 12-hr elliptic orbit. The effect

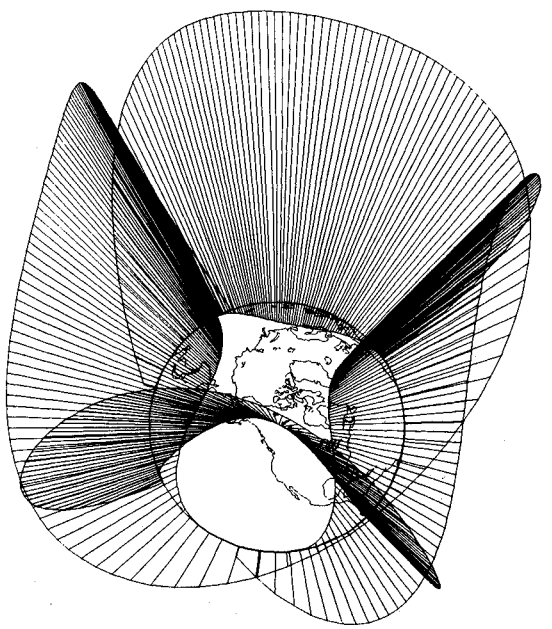

Fig. 2 Motion relative to the rotating Earth for a 6-hr elliptic orbit.

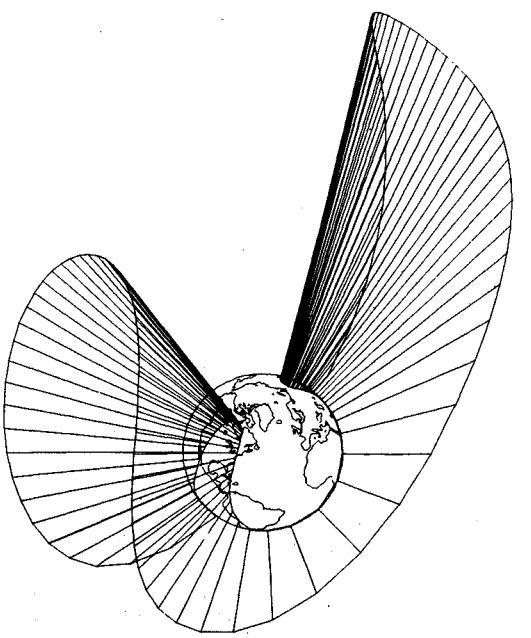

Fig. 4 Northern hemisphere view for a 12-hr elliptic orbit.

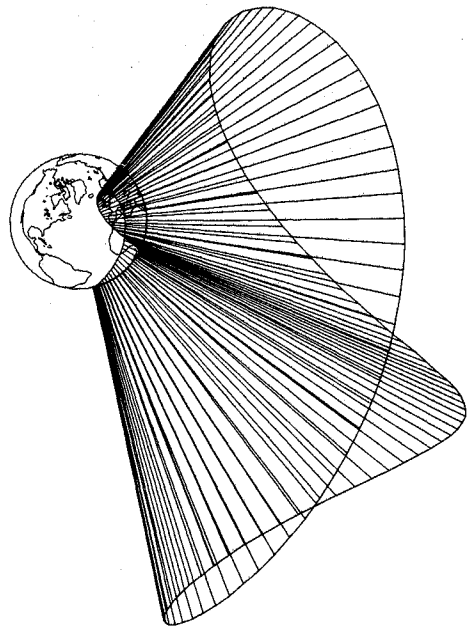

Fig. 5 Northern hemisphere view for a 24-hr elliptic orbit.

of Kepler's Second Law is quite visible in this figure. Finally, the motion of a 24-hr elliptic orbit of small eccentricity is shown in Fig. 5. This orbit essentially "rides" up and down the Greenwich meridian as a centerline and always remains on one side of the Earth.

Computer Program Discussion

The original computer program was developed by Baldwin[2] in the early sixties to display missile trajectories and satellite orbits relative to an Earth background. However, this code was first largely ignored because of its size, complexity, and a few residual "bugs" which caused a certain amount of havoc. Recently, the program's usefulness became apparent during several satellite system design studies and, later, for an actual Earth satellite experiment. Consequently, the existing code was modified and improved and many plots were computed by the author and his colleagues.[3-5]

The program is written in Fortran V and is presently running on a Univac 1108 Computer at Lockheed Missiles and Space Co. Depending upon the number of data points forming the orbit, each figure takes from 5 to 15 sec of computer time. In turn, a very large portion of this time is consumed in processing the coastline data and plotting the principal land masses and larger lakes which are visible from the selected viewpoint. For further information, the interested reader is referred to Madigan.[6]

In conclusion, the main purpose of this Note was to present, mostly for the reader's enjoyment, some of the more interesting illustrations which have been obtained during the last few years. A secondary purpose was to announce the existence of such a program to a wide audience.

Table 2 Pertinent plot data

Figure number	Viewpoint L, λ (deg)	Number of points
1	90.0, 0	500
2	60.0, −120.0	400
3	60.0, −120.0	300
4	45.0, −50.0	100
5	45.0, −45.0	100

References

[1] "Apollo 16 Brings Us Visions from Space," *National Geographic*, Vol. 142, No. 6, Dec. 1972, pp. 856–865.

[2] Baldwin, H. L., "Orbit Display Using the SC-4020," Rept. 63-0459, 1963, General Dynamics/Astronautics, San Diego, Calif.

[3] Hitzl, D. L., "Computer Graphics," Internal Note, Oct. 1969, Lockheed Palo Alto Research Lab., Palo Alto, Calif.

[4] Hitzl, D. L. and Shayer, S., "Computer Illustrations," Internal Note, Oct. 1969, Lockheed Palo Alto Research Lab., Palo Alto, Calif.

[5] Hitzl, D. L., "The Relative Motion of Commensurate Earth Satellites," Internal Note, Aug. 1971, Lockheed Palo Alto Research Lab., Palo Alto, Calif.

[6] Madigan, J. T., "Orbit Display Using the SC-4020 Subroutine MPLOT," Lockheed Missiles and Space Co., Sunnyvale, Calif., 1963.

Mean Flow Development and Surface Heating for an Attaching Compressible Free Shear Layer

DAVID H. RUDY* AND STANLEY F. BIRCH†

NASA Langley Research Center, Hampton, Va.

Introduction

HIGH surface heating rates encountered in regions of shock interference flows are important considerations in design of hypersonic vehicles such as space shuttle. Shock interference patterns have been classified by Edney[1] into six basic types. The present Note considers the interaction resulting when a weak extraneous shock wave impinges on the bow shock of a bluff body inside the sonic line, producing a single shear layer with supersonic flow on one side and subsonic on the other. This interaction, classified as type III by Edney, can occur between the mated booster and orbiter during the ascent phase of a shuttle mission.[2]

Previous experimental studies of type III interactions have been made by Edney[1] using several geometric shapes as bluff bodies and by Hains and Keyes[2,3] using a hemisphere. These studies provided surface heating and pressure data for various

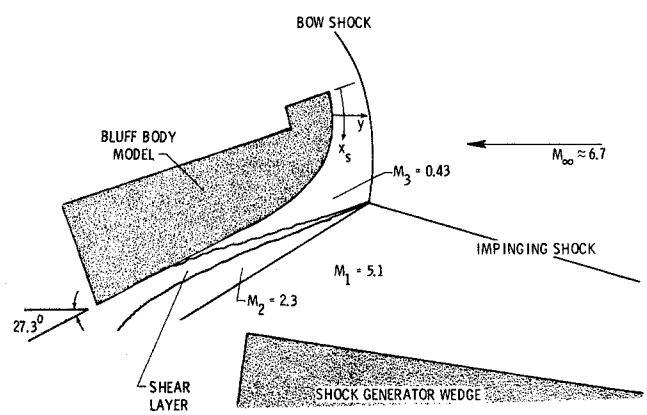

Fig. 1 Flowfield for a typical test condition.

Received September 10, 1973; revision received November 27, 1973.

Index categories: Supersonic and Hypersonic Flow; Jets, Wakes, and Viscid-Inviscid Flow Interactions.

* Aerospace Engineer, Analytical Fluid Mechanics Section, Hypersonic Vehicles Division.

† NASA-NRC Resident Research Associate, Hypersonic Vehicles Division; presently employed at The Boeing Company, Seattle, Wash.